Available online at www.sciencedirect.com

ScienceDirect

Energy Procedia 38 (2013) 658 – 669

Energy Procedia

SiliconPV: March 25-27, 2013, Hamelin, Germany

Numerical analysis of electrical TCO / a-Si:H(p) contact properties for silicon heterojunction solar cells

Martin Bivour*, Sebastian Schröer, Martin Hermle

Fraunhofer Institute for Solar Energy Systems ISE, Heidenhofstr. 2, 79110 Freiburg, Germany

Abstract

In this paper we present a one-dimensional numerical simulation study concerning the electrical properties of the TCO / a-Si:H(p) / a-Si:H(i) / c-Si(n) hole contact in amorphous / crystalline silicon heterojunction (SHJ) solar cells. Simulations where performed with Sentaurus TCAD from Synopsys considering the implemented barrier tunneling model. The modification of the a-Si:H(p) / a-Si:H(i) / c-Si(n) p/n junction by the opposing TCO / a-Si:H(p) junction and its influence on the device recombination for the relevant working conditions are investigated. We demonstrate the relevance of the effective screening length in the amorphous silicon, which depends on the effective space-charge in the a-Si:H(p) and the work function mismatch at the TCO / a-Si:H(p) interface. We highlight the importance of an improved work function matching as this presents an additional degree of freedom for the design of the SHJ and is an important parameter to reach both a very high V_{oc} and *FF*.

Keywords: silicon heterojunction; fill factor; tunneling; TCO; work function; loss analysis

1. Introduction

Owing to it´s ultra-low junction recombination silicon heterojunction (SHJ) solar cells have proven to be high efficiency devices [1], [2]. Especially for open-circuit (OC) conditions, junction recombination can be suppressed very efficiently so that device recombination is limited mainly by the intrinsic recombination of the high-quality crystalline silicon (c-Si) absorber, leading to very high open-circuit voltages (V_{oc}) of nearly 750 mV [1]. Consequently, an improved light management (higher J_{sc}) and a reduction of the losses under maximum power point (MPP) conditions (higher *FF*) are required to further

* Corresponding author. Tel.: +49-761-4588-5586; fax: +49-761-4588-9250.
E-mail address: martin.bivour@ise.fraunhofer.de.

doi:10.1016/j.egypro.2013.07.330

improve the device performance. In this respect a proper junction engineering of the SHJ at the illuminated front is of crucial importance, because a strong trade-off between the electrical and optical properties of both, the TCO electrode and the silicon thin films is observed.

Up to now, optimization of the TCO properties is limited mainly to the bulk properties. In this respect it has been shown that a high mobility TCO is mandatory at the front side to combine a high lateral conductivity (lateral transport to the metal grid electrode) and excellent optical properties [3], [4]. As most high mobility TCOs require process temperatures above 200°C [5] the choice of TCO materials seems to be limited to indium based materials for the front side as higher temperatures can cause a thermal induced degradation of the SHJ. However, concerning their interface properties, indium based materials might not be the best choice. Depending on the work function mismatch (ΔWF) between the contact materials, i.e. the TCO electrode and the doped silicon thin film, an opposing diode is formed which can strongly influence the device performance [6], [7], [8], [9], [10]. For amorphous silicon the work function of common TCO´s [11] is expected to be around mid-gap. Consequently, an opposing diode is formed for both p and n-doped material. The characteristics and the influence of this opposing diode on the silicon thin film / c-Si junction underneath is dominated by ΔWF as well as the doping and the thickness of the silicon thin film layer which is contacted by the TCO. However, the choice of thickness and doping of the silicon thin film layer is restricted: (i) an increased thickness of the silicon thin films will lower J_{sc} due to losses of the photo generation current with the absorber [12]. (ii) Highly-doped layers might not be applicable as a high doping can strongly interfere with the V_{oc} of the device. This fact can be explained mainly by a depassivation of the c-Si absorber surfaces, which is of importance especially for p-doping of the silicon thin films [13], [14]. (iii) A high (net) doping might not be possible, as in the case of silicon based thin film alloys. These materials are of interest because they are featuring better optical properties. However, in their amorphous structure typically a lower doping efficiency is observed [15]. The growth of ultra-thin materials featuring a significant crystalline fraction and thus the potential of higher doping efficiencies seems to be challenging for the illuminated front side of SHJ cells. This is attributed to the fact that typically an incubation layer of several nm is formed before material with a high crystalline fraction starts to grow. If this is the case, the optical thickness might be above the acceptable value. Degradation of the underlying buffer layer during growth of the doped overlayer seems to be another issue. Consequently, the restrictions on the interface work function between the TCO and the doped silicon thin film are high as an improved work function matching allows a lower doping and a lower thickness of the silicon thin films. Thus, the trade-off between doping (Fermi-level) induced defect formation (lowering the V_{oc}) and the TCO / doped silicon thin film contact properties (improving FF, V_{oc} and J_{sc}) should be less pronounced if the work function matching is improved.

In this paper, we concentrate on the influence of the interfacial work function at the TCO / doped silicon thin film interface (WF_{if}) and the net doping and the thickness of the doped silicon thin film on the device performance. In detail, numerical device simulations are performed for the TCO / a-Si:H(p) / a-Si:H(i) / c-Si(n) front contact of amorphous / crystalline silicon heterojunction solar cells.

2. Numerical modeling

One-dimensional numerical device simulations are performed with Sentaurus TCAD [16]. The Poisson and the continuity equations for electrons and holes are solved considering Shockley-Read-Hall recombination statistics for the a-Si:H and for the defect layer at the interface between a-Si:H and c-Si (D_{it}). For the bulk recombination of the 100 µm c-Si absorber only intrinsic recombination mechanisms (radiative and Auger) are considered. The layer and interface properties are summarized in the appendix. For simplicity, Fermi-level (E_f) and doping dependent defect formation [17], respectively, are not considered for the a-Si:H layers and the D_{it}. Thus, the doping variation of the a-Si:H(p) layer does not

modify the defect distribution and concentration of the doped and intrinsic a-Si:H films and of the D_{it}. Consequently, the experimentally often observed increase of junction recombination and decrease of V_{oc} with higher doping is not reflected within these simulations. Furthermore, the influence of the defect distribution and concentration of the a-Si:H on the TCO / doped silicon thin film contact properties [6], [18], is not taken into account. For the heterojunction between the doped a-Si:H and the TCO the exact band line-up is not reflected within these simulations as the TCO is not treated as an individual n-type semiconductor but as a "conductive" layer characterized only by its interface work function (WF_{if}), its bulk conductivity and the optical n, k values. We consider barrier tunnelling processes for the whole WF_{if} / a-Si:H(p) / a-Si:H(i) / c-Si(n) region. Because there is a high uncertainty about the value of WF_{if} and because this value will vary with the electrode material (ITO, AZO, etc.) and the chemical modifications of the interface during subsequent processing, etc., we perform a wide variation of WF_{if}. In the paper we will refer to both, WF_{if} and the work function mismatch $\Delta WF = WF_{if} - WF_{a\text{-}Si:H(p)} = WF_{if} - (E_{v,a\text{-}Si:H(p)} - E_{act})$ with $WF_{a\text{-}Si:H(p)}$, $E_{v,a\text{-}Si:H(p)}$ and E_{act} representing the work function, valence band energy and activation energy of the p-doped silicon thin film. For the doping variation a fixed $E_{v,a\text{-}Si:H(p)}$ is assumed. We chose activation energies of 200, 300 and 400 meV which correspond to an a-Si:H(p) WF of 5.4, 5.3 and 5.2 eV, respectively. These values are determined under equilibrium conditions without the influence of external contacts for the a-Si:H(p) layer. It should be noted, that 200 meV rather corresponds to a layer with very high doping (efficiency) which might be hard to achieve for purely amorphous p-layers [19],[20], whereas 400 meV presents a very low doping. Mainly for didactic reasons, we consider the case of semiconductor insulator semiconductor (SIS) cells where the doped a-Si:H layer is replaced by an additional intrinsic layer (E_{act} = mid-gap) and the contact properties are defined mainly by WF_{if}. This intrinsic layer is featuring either the bulk defects of the intrinsic buffer layer or of the defective doped layers. For the recombination at the TCO / doped silicon thin film interface a constant surface recombination velocity of $1 \cdot 10^7$cm/s for holes and electrons is assumed. For the a-Si:H(n) / WF_{if} rear contact, flat-band conditions and thus ohmic contact characteristics are assumed, which means that the WF_{if} is matched to the WF of the a-Si:H(n). A lumped series resistance of 0.4 Ωcm is assumed. Consequently, the variable input parameters for these simulation studies are (i) WF_{if}, (ii) $E_{act,a\text{-}Si:H(p)}$ and (iii) $t_{a\text{-}Si:H(p)}$ which corresponds to the thickness of a-Si:H(p) emitter.

3. Theoretical considerations

According to MIS and SIS solar cell theory [21] for the hole contact of a n-absorber, the work function of the p-electrode (metal, TCO or semiconductor) has a strong influence on the rectifying behaviour and the selectivity of the contact to holes or electrons, respectively. This is attributed mainly to the corresponding band bending resulting from the WF difference between the electrode and the absorber. In the case of $WF_{p\text{-}electrode} > WF_{c\text{-}Si(n)}$ this band bending leads to inversion conditions and consequently to the formation of a "pseudo" p/n junction near the interface within the absorber. Depending on the magnitude of this band bending a barrier for the majority carriers of the absorber (electrons) is formed. In the equilibrium case, this band bending is defined as the built-in potential ($V_{bi,c\text{-}Si}$) which is reduced by the external voltage under non equilibrium conditions. Consequently, a high $V_{bi,c\text{-}Si}$ is required to guarantee a sufficient selectivity of the contact for all working conditions. However, for typical silicon based heterojunction solar cells a semiconductor is applied as buffer layer instead of an insulator. Furthermore, between the TCO electrode and the buffer layer a doped silicon thin film is applied to increase $V_{bi,c\text{-}Si}$ as the WF of the doped silicon thin film is typically higher than that of the TCO electrode. Thus, for typical SHJ cells the doped a-Si:H(p) serves the purpose of the high WF electrode for the hole contact. However, the work function of the TCO electrode is still lower compared to that of the doped a-Si:H(p). This leads to $WF_{if} < WF_{a\text{-}Si:H(p)}$ and the band bending that results in the doped silicon thin film is opposed to $V_{bi,c\text{-}Si(n)}$.

An opposing diode with a corresponding $V_{bi,a\text{-}Si:H(p)}$ counteracting $V_{bi,c\text{-}Si(n)}$ is formed by the inappropriate WF induced by the TCO electrode. Consequently, three basic requirements have to be fulfilled to maximize $V_{bi,c\text{-}Si(n)}$ for a given $WF_{c\text{-}Si(n)}$. (i) a high $WF_{a\text{-}Si:H(p)}$. For a given silicon thin film this is obtained for low E_{act} and thus a high net doping. (ii) ΔWF should be small for the case of $WF_{if} < WF_{a\text{-}Si:H(p)}$ (ideally, $WF_{if} > WF_{a\text{-}Si:H(p)}$). Consequently, WF_{if} should be as high as possible for the hole contact. (iii) the doped layer has to provide an efficient screening of the opposing bend bending that originates from ΔWF. This is important because the penetration of the doped layer by $V_{bi,a\text{-}Si:H(p)}$ would lead to a reduction of $V_{bi,c\text{-}Si}$. If this is the case the a-Si:H(p) / a-Si:H(i) / c-Si(n) p/n junction properties would be dominated by WF_{if} (in a negative way) and not by the doped silicon thin film. For the sake of completeness it should be pointed out that experimentally a fourth important requirement, that is a low defect density for all layers and interfaces, can strongly interfere with a low E_{act}. However, as described in section two this fact is not reflected within the simulation. The importance of (ii) and (iii) can be deduced from the effective screening length [22]

$$L_{S,a-Si:H(p)} = 2 \cdot \sqrt{\frac{\varepsilon_0 \, \varepsilon_r \, k \, T}{2 \, q^2 \left| Q_{tot,a-Si:H(p)} \right|}} \cdot \sqrt{\frac{q \left| \Delta WF \right|}{k \, T}} \, ,$$

which defines the characteristic length that would be required to screen the band bending that results from ΔWF within the specific a-Si:H(p) layer. The first square-root corresponds to the Debye length and the second one corresponds to $V_{bi,a\text{-}Si:H(p)}$, e.g. ΔWF. $Q_{tot,a\text{-}Si:H(p)}$ is the total space charge density within the a-Si:H(p) at equilibrium conditions obtained from integration over the a-Si:H(p) layer. It is defined by the charge of the free carriers, trapped charges and the charges of ionized doping impurities. The other parameters have their usual meaning. Consequently, for $t_{a\text{-}Si:H(p)} > L_{s,a\text{-}Si:H(p)}$ the negative influence of this opposing band banding is limited to the a-Si:H(p) layer. In this case a direct influence on $V_{bi,c\text{-}Si}$ and, thus, on the p/n junction properties is not observed. For the non equilibrium conditions a sufficient small $L_{s,a\text{-}Si:H(p)}$ guarantees an efficient tunneling of holes from the a-Si:H(p) into the TCO electrode. This is attributed to the corresponding decrease of the barrier width which will reduce the effective barrier height [23] for holes at the a-Si:H(p) / TCO interface. An efficient tunneling prevents the pile up of holes in the p-layer which would lead to a further reduction of the negative $Q_{tot,a\text{-}Si:H(p)}$ by the positive charges of the free holes for non equilibrium conditions. A pile up of holes and the reduction of $Q_{tot,a\text{-}Si:H(p)}$ would cause an additional reduction of the band bending in the absorber for a given external voltage. Consequently, the selectivity of the contact is lowered for the respective working condition. Around the MPP this effect seems to be most pronounced as the band bending of the absorber is already significantly reduced by the external voltage and the current density at the TCO / a-Si:H(p) interface is still high, causing a pile up of holes if tunneling is inefficient.

4. Results

4.1. Critical a-Si:H(p) thickness

Fig. 1 shows the influence of $t_{a\text{-}Si:H(p)}$ for very high (E_{act} = 200 meV) and very low (E_{act} = 400 meV) net doping on the effective screening length, $V_{bi,c\text{-}Si}$ and the cell output parameters. A constant WF_{if} of 4.9 eV was assumed for both activation energies, leading to a work function mismatch of 500 and 300 meV for

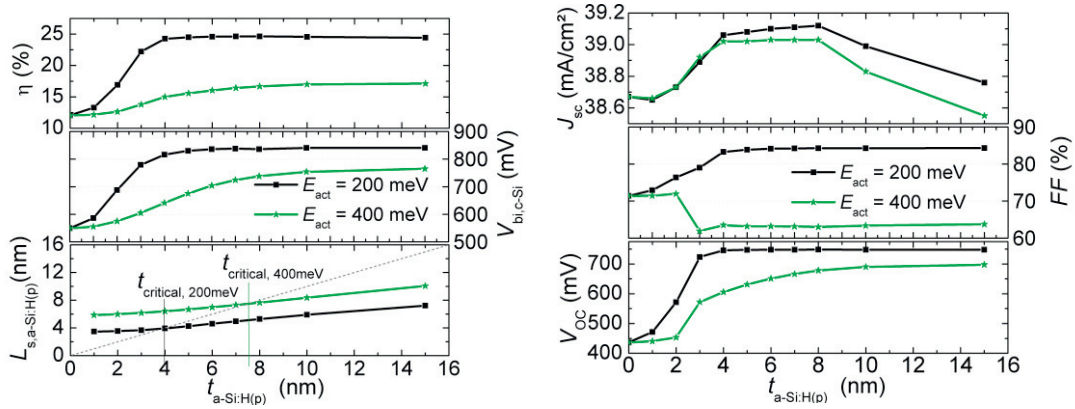

Fig. 1: Influence of the thickness of the p-layer ($t_{a\text{-}Si:H(p)}$) for activation energies of E_{act} = 200 meV (black lines) and E_{act} = 400 meV (green lines) on the effective screening length, $V_{bi,c\text{-}Si}$ and the cell efficiency, as well as on the output parameters V_{OC}, *FF* and J_{SC}, for an WF_{if} of 4.9 eV.

the very high and very low a-Si:H(p) net doping, respectively (increase of ΔWF with net doping). The relevance of $V_{bi,c\text{-}Si}$ for an optimal device performance can clearly be seen. It can be seen that for the case of $t_{a\text{-}Si:H(p)} < L_{s,a\text{-}Si:H(p)}$ the built-in voltage $V_{bi,c\text{-}Si}$ as well as the V_{oc} are strongly reduced for both activation energies. For the high net doping a comparable behavior for both, the V_{oc} and *FF* is observed. The simulated output parameters for the highly-doped layers are in good qualitative agreement with experimental data where for an ITO electrode a thickness variation of the p-emitter was performed [24],[25],[12]. In the latter two publications the critical thickness of the p-layer up to which a significant influence on the V_{oc} and *FF* is observed amounts to about 3 and 5 nm. The simulated data for the case of very low doping (E_{act} = 400 meV) are not reflected by these experimental investigations as a different *FF* dependence and much lower *FF* and V_{oc} values are observed in the simulation study. According to the results of Fig. 1, an activation energy of the p-layer of well below 400 meV seems to be mandatory to guarantee sufficient $V_{bi,c\text{-}Si}$. The importance of $V_{bi,c\text{-}Si}$ for the V_{oc} and its interplay with the absorber passivation by the SHJ is experimentally investigated in [26]. Another approach to experimentally characterize the V_{oc} losses induced by insufficient doping is presented in [27]. The influence of both, the doping and thickness on the V_{oc} is investigated in [28] where it is experimentally shown that higher doping leads to a reduction of the critical thickness. In real devices partial shortening of the junction by local thickness variations of the silicon thin film (for non-planar / textured surfaces) or additional transport channels not considered in the simulation (i.e. hopping via gap/tail states) and the recombination at the TCO / doped silicon thin film interface might be other issues for very thin layers.

4.2. Influence of the work function mismatch

Fig. 2 demonstrates the interplay between the WF_{if}, the a-Si:H(p) doping and a-Si:H(p) thickness and its influence on the cell performance. It can be seen that for very high WF_{if} the best cell results are observed. This is attributed to the fact that for a positive ΔWF ($WF_{if} > WF_{a\text{-}Si:H(p)}$) the band bending at the TCO / a-Si:H(p) interface which originates from ΔWF leads to accumulation conditions in the a-Si:H supporting $V_{bi,c\text{-}Si}$. Thus, WF_{if} dominates the p/n junction properties in a positive manner. Even though

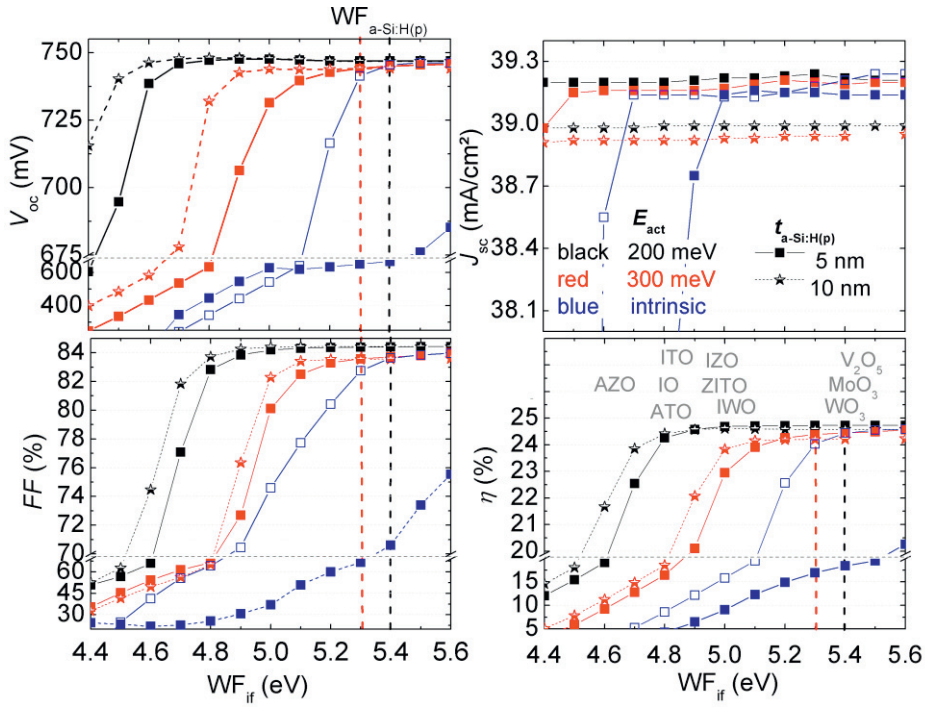

Fig. 2: V_{OC}, FF, J_{SC} and the efficiency as a function of WF_{if} for different a-Si:H(p) doping and a-Si:H(p) thicknesses.

this is highly desirable it is questionable if such high WF_{if} can be reached for real devices. For the flat band case ($WF_{if} = WF_{a\text{-}Si:H(p)}$) the p/n junction properties are determined solely by the a-Si:H. Consequently, the highest efficiencies are observed for the highest doping and $WF_{a\text{-}Si:H(p)}$, respectively.

As demonstrated in the previous section, for a negative work function mismatch ($WF_{if} < WF_{a\text{-}Si:H(p)}$) the influence of the opposing diode can degrade the device performance as for this case a local or global depletion of the a-Si:H is observed. It can clearly be seen that for very high doping a very large ΔWF can be tolerated. For all E_{act} an increase of V_{oc} and FF is observed if the a-Si:H(p) thickness is increased from 5 to 10 nm. A further improvement for 15 nm is not observed (not shown). Consequently, it is expected that for all doped layers and all WF_{if} the critical thickness is smaller than 10 nm.

The MIS or SIS like cells with an intrinsic 5 nm "a-Si:H(p)" layer (blue curves) show the strongest dependence on WF_{if} which demonstrates that very high WF_{if} would be required to reach reasonable efficiencies for this type of solar cell. This is especially true for the cells featuring an intrinsic a-Si:H layer with the defect density and characteristics of the p-layers (blue curves, solid squares). Comparing these results to the cells with the less defective intrinsic a-Si:H layer (blue curves, open squares), the importance of SRH recombination within the a-Si:H and at the interface to the TCO in dependence on WF_{if} and the corresponding degree of depletion can be deduced (further discussed in the next section). Consequently, good SIS cells would theoretically be possible if a very high WF_{if} and a low defect density near the interface could be guaranteed. In an experimental paper [29] we have studied the influence of the WF_{if} on the V_{oc} for such devices. As shown in previous investigations [21] the expected strong dependence of WF_{if} on V_{oc} was experimentally observed. We showed that for an ITO electrode, which is the typical electrode applied to SHJ cells, the V_{oc} is below 400 mV. According to the results of Fig. 2 this corresponds to a WF_{if} of well below 5 eV. This fact clearly demonstrates the inappropriate WF_{if} that is

introduced by the ITO electrode. Thus, further device optimization should include the engineering of $WF_{if.}$ This is presented in [30] for a variation of the a metal electrode and the a-Si:H(p) doping for rear emitter cells. The application of interfacial high WF layers is well known from other devices including thin film solar cells [31], organic [32],[33] and MIS devices [34]. Thus, the relevance of WF_{if} for SHJ solar cells should be experimentally investigated further too, to gain a comprehensive understanding of the SHJ junction properties.

A comparison between the results of Fig. 2 (where $WF_{if} < WF_{a\text{-}Si:H(p)}$) and the experimentally observed behavior from literature [2] leads to the conclusion that only a sufficient high doping with activation energies of 300 and 200 meV leads to the - for SHJ cells typical - very high V_{oc} of well above 700 mV. For activation energies of above 300 mV (not shown) the V_{oc} is strongly reduced by the insufficient $V_{bi,c\text{-}Si}$ as shown in Fig. 1 for an E_{act} of 400 meV and WF_{if} of 4.9 eV. Consequently, for real devices the influence of WF_{if} on the V_{oc} is expected to be moderate. In other words, doping and the ΔWF are sufficient to allow an acceptable selectivity at OC as demonstrated by the high V_{oc} typically observed for SHJ cells. However, the restrictions on doping and the ΔWF are much higher under MPP conditions. For a high *FF* of above 80 % higher doping and higher WF_{if} are required. According to this simulation, E_{act} has to be below 300 meV to achieve satisfying *FF* (and V_{oc}) with WF_{if} below 5eV. However, in real devices the applicable doping and E_{act} will define the lower limit of WF_{if}. In the literature a wide variation of work functions for the nominal same TCO material can be found [11], [35]. This can be attributed to both, the difference in the fabrication and the interfacial TCO properties. A very rough indication of the WF is given in Fig. 2 for different TCO materials. It should be noted that the effective WF that results after contact formation between the TCO and doped silicon thin film (WF_{if}) can differ substantially from these values that are determined for the TCO in contact to vacuum or air [11], [35]. However, it can clearly be seen that the application of high WF TCOs at the interface would considerable increase the degrees of freedom for the design of the silicon thin film part of the junction, i.e. allow the application of thinner and less doped layers. For the real device this would allow *FF* and J_{sc} improvements without compromising the V_{oc}, leading to an increase of the efficiency.

4.3. Specific device recombination

In Fig. 3 we have plotted the total and layer specific device recombination in dependence of the external terminal voltage for two cells from Fig. 2 featuring a 5 nm thick a-Si:H(p) emitter and activation energies of 200 and 300 meV. On the left hand side a WF_{if} of 4.9 eV and on the right hand side a WF_{if} of 5.0 eV are assumed. Starting with the cells featuring a very high doping with E_{act} of 200 meV (black lines) it can be seen that under OC conditions Auger recombination in the c-Si absorber is the dominant recombination path. Under MPP conditions the (SRH) recombination in the a-Si:H(p) layer and at the a-Si:H(i) / c-Si(n) interface defects becomes more relevant. However, the total device recombination is still on a low level. Consequently, very high V_{oc} and *FF* values can be reached for both WF_{if} as shown in Tab. 1. It should be mentioned that the dotted lines in Fig. 3 correspond not only to the SRH recombination in the bulk of p-emitter but also to recombination at the TCO / a-Si:H(p) interface. The latter corresponds to about 60 % of the recombination losses of the highly doped 5 nm p-emitter (dotted line). In the case of a lowly doped emitter with E_{act} of 300 meV (red lines), the device recombination is strongly increased for MPP as well as OC conditions. Thus, the *FF* and V_{oc} are significantly reduced compared to the highly doped emitter as can be seen in Tab. 1. Especially for the higher ΔWF and WF_{if} of

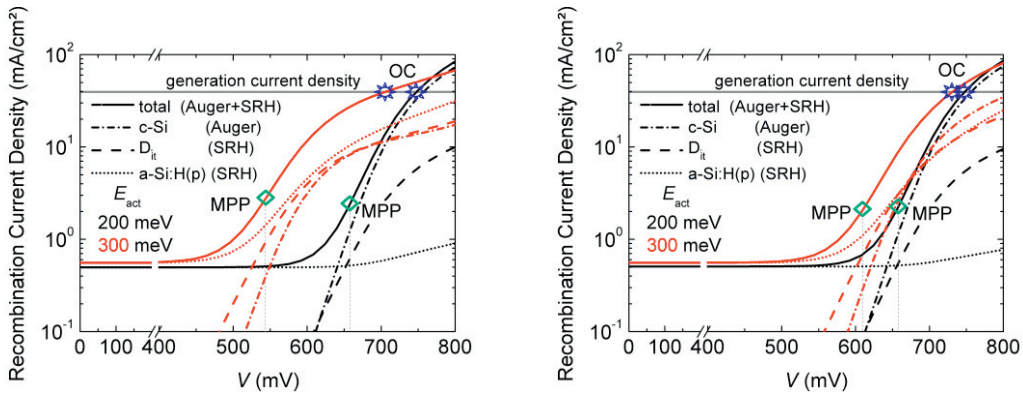

Fig. 3: Total and layer specific recombination as a function of the external voltage for a WF_{if} of 4.9 eV (left) and a WF_{if} of 5.0 eV (right).

4.9 eV a significant reduction of the efficiency is observed. It can clearly be seen that due to the lower p-doping the dominant device recombination at MPP is changed from Auger recombination in the crystalline absorber to SRH recombination in the depleted a-Si:H(p) bulk and at the depleted TCO / a-Si:H(p) interface of the p-emitter. In this case, the latter amounts to only 30 % of the recombination losses as mainly the recombination in the a-Si:H(p) bulk is increased by the lower doping. Furthermore, SRH recombination at the a-Si:H(i) / c-Si(n) interface defects becomes significant too. For the better work function matching (WF_{if} 5.0 eV) the increase in SRH recombination is less pronounced leading to high efficiencies despite the moderate a-Si:H(p) doping. Thus, according to this recombination analysis it becomes obvious that an improved work function matching is important to reach both a high V_{oc} and *FF* especially when the applicable doping is limited. In conclusion, the lower p-doping leads to an insufficient screening of the opposing TCO / a-Si:H(p) junction from the a-Si:H(p) / a-Si:H(i) / c-Si(n) p/n junction. Two effects interact and cause the increased (SRH) recombination under MPP and OC conditions. Depending on the effective screening length (i) the built-in potential in the crystalline part of the p/n junction ($V_{bi,c\text{-}Si}$) is reduced leading to a less selective a-Si:H / c-Si p/n junction for all working conditions (and applied voltages). The concentration of the electrons (minority carriers) is increased in the p/n junction region. (ii) the lower doping leads to a wider tunneling barrier for the holes at the TCO/a-Si:H(p) contact. The tunneling through this barrier becomes less efficient and the holes (majority carriers) begin to pile up in the p/n junction region. Together with the higher electron concentration this leads to an increased SRH recombination in the defective and depleted p-emitter region for both, MPP and OC conditions.

Table 1. Cell output parameter for the cells from Fig. 3

WF_{if} (eV)	E_{act} (meV)	J_{SC} (mA/cm²)	V_{OC} (mV)	J_{MPP} (mA/cm²)	V_{MPP} (mV)	*FF* (%)	η (%)
4.9	200	39.3	748	37.5	656	83.9	24.6
5	200	39.3	748	37.7	656	84.2	24.7
4.9	300	39.2	706	37.0	544	72.7	20.1
5	300	39.2	731	37.8	608	80.1	23.0

5. Conclusion and outlook

We have demonstrated the influence of the interfacial work function at the TCO / doped silicon thin film contact, the silicon thin film net doping and the silicon thin film thickness on the selectivity of the hole contact of amorphous / crystalline silicon heterojunction solar cells for the relevant working conditions. It has been shown that the application of high WF TCOs at the interface or other approaches that result in a higher interface work function would considerably increase the degrees of freedom for the design of the SHJ junction, i.e. allow the application of thinner and less doped silicon thin films. For further improvements of the device simulation the experimentally observed increase of device recombination with higher silicon thin film doping has to be considered. Furthermore, the TCO electrode should be described as individual semiconductor layer and not "only" as a metal contact layer featuring a certain work function. In this case the transport at the TCO / doped silicon thin film heterojunction should be determined not only by the work function but also by the band line up at the interface.

Acknowledgments

The authors would like to thank C. Reichel and F. Feldmann for helpful discussions. This work was funded by the German Federal Ministry for the Environment, Nature Conservation and Nuclear Safety under contract number 0325292''ForTeS''. Martin Bivour gratefully acknowledges the scholarship support from the Reiner Lemoine Stiftung.

References

[1] T. Kinoshita, D. Fujishima, A. Yano, et al., The approaches for hig efficiency HIT (trademark) solar cell with very thin (<100μm) silicon wafer over 23%, *in Proceedings of the 26th European Photovoltaic Solar Energy Conference and Exhibition*, Hamburg, Germany, 2011 871-4.

[2] S. De Wolf, A. Descoeudres, Z. C. Holman, et al., High-efficiency Silicon Heterojunction Solar Cells: A Review, *green* 2012; **0**.

[3] T. Koida, H. Fujiwara and M. Kondo, Reduction of Optical Loss in Hydrogenated Amorphous Silicon/Crystalline Silicon Heterojunction Solar Cells by High-Mobility Hydrogen-Doped In2O3 Transparent Conductive Oxide, *Applied Physics Express* 2008; **1** 041501.

[4] L. Barraud, Z. C. Holman, N. Badel, et al., Hydrogen-doped indium oxide/indium tin oxide bilayers for high-efficiency silicon heterojunction solar cells, *Solar Energy Materials and Solar Cells* 2013; **115** 151-156.

[5] S. Calnan and A. N. Tiwari, High mobility transparent conducting oxides for thin film solar cells, *Thin Solid Films* 2010; **518** 1839-1849.

[6] J. K. Arch, F. A. Rubinelli, J.-Y. Hou, et al., Computer analysis of the role of p-layer quality, thickness, transport mechanisms, and contact barrier height in the performance of hydrogenated amorphous silicon p-i-n solar cells, *Journal of Applied Physics* 1991; **69** 7057-7066.

[7] R. Stangl, A. Froitzheim, M. Schmidt, et al., Design criteria for amorphous/crystalline silicon heterojunction solar cells - a simulation study, *in Proceedings of the 3rd World Conference on Photovoltaic Energy Conversion*, Osaka, Japan, 2003 1005-8.

[8] M. Schmidt, A. Froitzheim, R. Stangl, et al., Photocurrent analysis TCO/a-Si:H/c-Si solar cell structures *in Proceedings of the 17th European Photovoltaic Solar Energy Conference and Exhibition*, Munich, Germany, 2001 1383.

[9] A. Kanevce and W. K. Metzger, The role of amorphous silicon and tunneling in heterojunction with intrinsic thin layer (HIT) solar cells, *Journal of Applied Physics* 2009; **105** 094507.

[10] S. M. d. Nicolás, D. Muñoz, A. S. Ozanne, et al., Optimisation of doped amorphous silicon layers applied to heterojunction solar cells, *Energy Procedia* 2011; **8** 226-231.

[11] A. Klein, C. Körber, A. Wachau, et al., Transparent Conducting Oxides for Photovoltaics: Manipulation of Fermi Level, Work Function and Energy Band Alignment, *Materials* 2010; **3** 4892-4914.

[12] Z. C. Holman, A. Descoeudres, L. Barraud, et al., Current Losses at the Front of Silicon Heterojunction Solar Cells, *Photovoltaics, IEEE Journal of* 2012; **2** 7-15.

[13] S. De Wolf and M. Kondo, Nature of doped a-Si:H/c-Si interface recombination, *Journal of Applied Physics* 2009; **105** 103707.

[14] T. F. Schulze, C. Leendertz, N. Mingirulli, et al., Impact of Fermi-level dependent defect equilibration on Voc of amorphous/crystalline silicon heterojunction solar cells, *Energy Procedia* 2011; **8** 282-287.

[15] D. Muñoz, T. Desrues, A.-S. Ozanne, et al., Key aspects on development of high efficency heterojunction and IBC heterojunction solar cells: towards 22% efficency on industrial size, *in Proceedings of the 27th EUPVSEC, Frankfurt, Germany*, 2012.

[16] Synopsis, Zurich, Switzerland, Sentaurus Device Manual, 2012, (www.www.synopsis.com).

[17] M. Powell and S. Deane, Improved defect-pool model for charged defects in amorphous silicon, *Physical Review B* 1993; **48** 10815-10827.

[18] R. Varache, J. P. Kleider, M. E. Gueunier-Farret, et al., Silicon heterojunction solar cells: Optimization of emitter and contact properties from analytical calculation and numerical simulation, *Materials Science and Engineering: B* 2013; **178** 593-598.

[19] M. Stutzmann, D. Biegelsen and R. Street, Detailed investigation of doping in hydrogenated amorphous silicon and germanium, *Physical Review B* 1987; **35** 5666-5701.

[20] W. E. Spear and P. G. Le Comber, Substitutional doping of amorphous silicon, *Solid State Communications* 1975; **17** 1193-6.

[21] J. Shewchun, D. Burk and M. B. Spitzer, MIS and SIS solar cells, *Electron Devices, IEEE Transactions on* 1980; **27** 705-716.

[22] S. M. Sze, *Physics of semiconductor devices*, 2nd ed. New York: John Wiley & Sons, Inc., 1981.

[23] W. Jackson, R. Nemanich, M. Thompson, et al., Schottky barriers on phosphorus-doped hydrogenated amorphous silicon: The effects of tunneling, *Physical Review B* 1986; **33** 6936-6945.

[24] M. W. M. van Cleef, F. A. Rubinelli, J. D. Ouwens, et al., Amorphous-crystalline heterojunction silicon solar cells with an a-SiC:H window layer, *in Proceedings of the 13th European Photovoltaic Solar Energy Conference* Nice, France, 1995 1303-06.

[25] H. Fujiwara and M. Kondo, Effects of a-Si:H layer thicknesses on the performance of a-Si:H/c-Si heterojunction solar cells, *Journal of Applied Physics* 2007; **101** 054516.

[26] L. Korte, E. Conrad, H. Angermann, et al., Advances in a-Si:H/c-Si heterojunction solar cell fabrication and characterization, *Solar Energy Materials and Solar Cells* 2009; **93** 905-910.

[27] D. Pysch, C. Meinhard, N.-P. Harder, et al., Analysis and optimization approach for the doped amorphous layers of silicon heterojunction solar cells, *Journal of Applied Physics* 2011; **110** 094516.

[28] D. Pysch, C. Meinhardt, M. Hermle, et al., Development and understanding of the intrinsic and doped amorphous emitter-layer stacks for silicon heterojunction solar cells, *in Proceedings of the 25th European Photovoltaic Solar Energy Conference and Exhibition*, Valencia, Spain, 2010 1820-4.

[29] M. Bivour, C. Reichel, M. Hermle, et al., Improving the a-Si:H(p) rear emitter contact of n-type silicon solar cells, *Solar Energy Materials and Solar Cells* 2012; **106** 11-16.

[30] T. Desrues, P. J. Ribeyron, A. Vandeneynde, et al., B-doped a-Si:H contact improvement on silicon heterojunction solar cells and interdigitated back contact structure, *physica status solidi (c)* 2010; **7** 1011-1015.

[31] J. Kim, A. Abou-Kandil, K. Fogel, et al., The Role of High Work-Function Metallic Nanodots on the Performance of a-Si:H Solar Cells: Offering Ohmic Contact to Light Trapping, *ACS Nano* 2010; **4** 7331-7336.

[32] S. Chen, J. R. Manders, S.-W. Tsang, et al., Metal oxides for interface engineering in polymer solar cells, *Journal of Materials Chemistry* 2012; **22** 24202.

[33] T. J. Marks, J. G. C. Veinot, J. Cui, et al., Progress in high work function TCO OLED anode alternatives and OLED nanopixelation, *Synthetic Metals* 2002; **127** 29-35.

[34] Y.-C. Yeo, T.-J. King and C. Hu, Metal-dielectric band alignment and its implications for metal gate complementary metal-oxide-semiconductor technology, *Journal of Applied Physics* 2002; **92** 7266.

[35] T. Minami, T. Miyata and T. Yamamoto, Work function of transparent conducting multicomponent oxide thin films prepared by magnetron sputtering, *Surface and Coatings Technology* 1998; **108–109** 583-587.

Appendix

	a-Si:H(p)	***a-Si:H(i)***	***a-Si:H(n)***	***c-Si(n)***	***"TCO"***
Thickness [μm]	varied	0.005	0.01	100	0.07
Electron Affinity [eV]	3.9	3.9	3.9	4.05	--
Bandgap [eV]	1.68	1.72	1.72	1.18	--
Work function [eV]	varied	4.7	4.10	4.32	varied
Activation Energy [meV]	varied	854	202	267	--
Electron/Hole Mobility [$cm^2/(Vs)$]	5/1	5/1	5/1	1500/450	--
Doping Concentration [$1/cm^3$]	varied	0	$7.8 \cdot 10^{19}$	$9.2 \cdot 10^{14}$	--
Effektive DOS CB [$1/cm^3$]	$1 \cdot 10^{20}$	$1 \cdot 10^{20}$	$1 \cdot 10^{20}$	$3.2 \cdot 10^{19}$	--
Effektive DOS VB [$1/cm^3$]	$1 \cdot 10^{20}$	$1 \cdot 10^{20}$	$1 \cdot 10^{20}$	$1.8 \cdot 10^{19}$	--
Electron/Hole Tunneling Mass [m_0]	0.1/0.35	0.1/0.35	0.1/0.35	0.3/0.55	0.5/0.5
DB Defect Concentration [$1/cm^3$]	$1.31 \cdot 10^{20}$	$1.39 \cdot 10^{16}$	$1.31 \cdot 10^{20}$	--	--
Energetic Position Acceptor-like DBs [eV]	1.1	0.89	0.5	--	--
Energetic Position Donor-like DBs [eV]	1.2	1.09	0.7	--	--
Capture Cross-Section Majority Carriers [cm^2]	$3 \cdot 10^{-14}$	$3 \cdot 10^{-14}$	$3 \cdot 10^{-14}$	--	--
Capture Cross-Section Minority Carriers [cm^2]	$3 \cdot 10^{-15}$	$3 \cdot 10^{-15}$	$3 \cdot 10^{-15}$	--	--
CB Tail Defect Concentration [$1/cm^3$]	$2 \cdot 10^{21}$	$1.88 \cdot 10^{21}$	$2 \cdot 10^{21}$	--	--

VB Tail Defect Concentration [$1/cm^3$]	$2 \cdot 10^{21}$	$1.88 \cdot 10^{21}$	$2 \cdot 10^{21}$	--	--
Capture Cross-Section Majority Carriers [cm^2]	$7 \cdot 10^{-16}$	$7 \cdot 10^{-16}$	$7 \cdot 10^{-16}$	--	--
Capture Cross-Section Minority Carriers [cm^2]	$7 \cdot 10^{-16}$	$7 \cdot 10^{-16}$	$7 \cdot 10^{-16}$	--	--